

RESEARCH LETTER

10.1002/2013GL058872

Key Points:

- Minimum sea ice albedo is too high in HadCM3 for mid-Pliocene simulations
- A lower minimum produces large high-latitude temperature increases
- Small reduction achieved in mismatch between model and data temperatures

Supporting Information:

- Readme
- Figures S1–S8
- Table S1
- Table S2

Correspondence to:

F. W. Howell,
eefwh@leeds.ac.uk

Citation:

Howell, F. W., A. M. Haywood, A. M. Dolan, H. J. Dowsett, J. E. Francis, D. J. Hill, S. J. Pickering, J. O. Pope, U. Salzmann, and B. S. Wade (2014), Can uncertainties in sea ice albedo reconcile patterns of data-model discord for the Pliocene and 20th/21st centuries?, *Geophys. Res. Lett.*, *41*, 2011–2018, doi:10.1002/2013GL058872.

Received 14 JAN 2014

Accepted 20 FEB 2014

Accepted article online 24 FEB 2014

Published online 20 MAR 2014

Can uncertainties in sea ice albedo reconcile patterns of data-model discord for the Pliocene and 20th/21st centuries?

Fergus W. Howell¹, Alan M. Haywood¹, Aisling M. Dolan¹, Harry J. Dowsett², Jane E. Francis^{1,3}, Daniel J. Hill^{1,4}, Steven J. Pickering¹, James O. Pope¹, Ulrich Salzmann⁵, and Bridget S. Wade⁶

¹School of Earth and Environment, University of Leeds, Leeds, UK, ²US Geological Survey, Reston, Virginia, USA, ³British Antarctic Survey, Cambridge, UK, ⁴Climate Change Programme, British Geological Survey, Nottingham, UK, ⁵Department of Geography, Faculty of Engineering and Environment, Northumbria University, Newcastle upon Tyne, UK, ⁶Department of Earth Sciences, University College London, London, UK

Abstract General Circulation Model simulations of the mid-Pliocene warm period (mPWP, 3.264 to 3.025 Myr ago) currently underestimate the level of warming that proxy data suggest existed at high latitudes, with discrepancies of up to 11°C for sea surface temperature estimates and 17°C for surface air temperature estimates. Sea ice has a strong influence on high-latitude climates, partly due to the albedo feedback. We present results demonstrating the effects of reductions in minimum sea ice albedo limits in general circulation model simulations of the mPWP. While mean annual surface air temperature increases of up to 6°C are observed in the Arctic, the maximum decrease in model-data discrepancies is just 0.81°C. Mean annual sea surface temperatures increase by up to 2°C, with a maximum model-data discrepancy improvement of 1.31°C. It is also suggested that the simulation of observed 21st century sea ice decline could be influenced by the adjustment of the sea ice albedo parameterization.

1. Introduction

The mid-Pliocene warm period (mPWP), covering the interval between 3.264 and 3.025 Myr ago [Dowsett *et al.*, 2010], was a period of sustained global warmth, when global annual mean temperatures are estimated to have been 2 to 3°C warmer than the present day [Haywood and Valdes, 2004], an increase within the warming range predicted by the Intergovernmental Panel on Climate Change for the end of the 21st century [Intergovernmental Panel on Climate Change, 2007]. Estimates of $p\text{CO}_2$ fall in the range of 365–415 ppm [Pagani *et al.*, 2010; Seki *et al.*, 2010]. General Circulation Model (GCM) simulations of mid-Pliocene climates do not produce the level of high-latitude warming, particularly in the North Atlantic and Arctic regions, implied by the proxy data [Dowsett *et al.*, 2011; Haywood *et al.*, 2013; Salzmann *et al.*, 2013].

Sea ice exerts a strong influence over high-latitude climates, particularly in the Arctic, through acting as an insulating cover between the ocean and the atmosphere, and its ability to amplify small changes through feedback mechanisms [Kellogg, 1975; Maykut, 1978], such as the albedo feedback, which can cause the amplification of an initial warming or cooling perturbation to the system [Curry *et al.*, 1995].

Sea ice albedo has often been used as a tuning mechanism in GCMs so that simulated sea ice extents and thicknesses have better agreement with modern observations [Eisenman *et al.*, 2008; Hunke, 2010]. Since values in GCMs are tuned with respect to the present day, they may not remain valid for simulating radically different climate states that existed in the past. This may also have implications for the validity of model predictions of global change. As proxy data indicate that high-latitude surface air and sea surface temperatures (SATs and SSTs) were several degrees warmer in the mid-Pliocene [Dowsett *et al.*, 2011; Haywood *et al.*, 2013; Salzmann *et al.*, 2013], it is likely that in comparison to the present day, less winter ice cover would survive the summer. Data from ostracode assemblages and ice-rafted debris sediments in the Arctic Basin suggest the presence of seasonal rather than perennial sea ice in the Pliocene Arctic [Cronin *et al.*, 1993; Moran *et al.*, 2006; Polyak *et al.*, 2010].

Arctic summer sea ice extent has declined dramatically in the last 30 years [Stroeve *et al.*, 2007; Comiso *et al.*, 2008], resulting in a shift toward increasing levels of first-year sea ice (ice formed after the end of the most recent melt season). GCMs have not successfully reproduced this decline and have generally overestimated

Arctic sea ice extent, particularly for the recent rapid decline [Stroeve *et al.*, 2007, 2012]. This may have implications for forecast simulations of the 21st century sea ice, if the models have been tuned with respect to a climate with more multiyear Arctic sea ice (ice that has survived at least one summer melt season).

Perovich et al. [2007] and *Perovich and Polashenski* [2012] have provided observations demonstrating the evolution of multiyear and first-year sea ice albedos throughout the summer. Multiyear sea ice albedo is shown to fall from a maximum of 0.85 to a minimum of ~ 0.4 just before the onset of freezeup. In contrast, first-year ice albedo can be as low as 0.2 and is less than multiyear ice albedo for most of the summer, never at any point exceeding it.

A large contribution to the difference in minimum albedo is the more extensive melt pond coverage on first-year ice [Polashenski *et al.*, 2012; Perovich and Polashenski, 2012]. The difference between first-year and multiyear sea ice questions whether a minimum albedo value tuned for modern climate is appropriate for an Arctic with a higher proportion of first-year ice than the present day.

This paper explores whether reducing the minimum sea ice albedo limit in the Hadley Centre Coupled Climate Model version 3 (HadCM3), in accordance with that expected from a higher proportion of first-year ice, could improve model-data agreement at high latitudes for the mid-Pliocene warm period. We focus only on the sea ice albedo in order to better quantify the effects with regard to the observations in *Perovich and Polashenski* [2012]. We also examine the response of September Arctic sea ice extent to albedo limit changes for modern transient simulations. If a lower minimum albedo can better reproduce the recent trend of sea ice decline, then as recent observations highlight a shift toward seasonal rather than perennial sea ice, this could reinforce the case for its use in simulations of warmer climates such as the mid-Pliocene.

2. Methods

2.1. Model Description

The model used in this study was HadCM3, a coupled atmosphere-ocean GCM produced by the UK Met Office Hadley Centre. In addition to the atmosphere and ocean, HadCM3 also contains vegetation and sea ice components [Gordon *et al.*, 2000].

The atmosphere component of HadCM3 has a horizontal resolution of $2.5^\circ \times 3.75^\circ$ (latitude \times longitude), which at the equator gives a grid box representing 278 km \times 419 km, and composes of 19 vertical levels [Gordon *et al.*, 2000]. The horizontal grid resolution of the ocean component is $1.25^\circ \times 1.25^\circ$, giving six ocean grid boxes for every atmosphere box, with 20 vertical levels. Coupling occurs once per day in the model run, with the forcing fluxes accumulating every 30 min model time step [Gordon *et al.*, 2000].

The sea ice model utilizes parameterizations of ice drift and leads alongside a basic thermodynamic scheme [Cattle and Crossley, 1995]. Semtner [1976] provides the basis for the thermodynamics of the model, and ice concentration parameterization is based on Hibler [1979]. The model also utilizes a sea ice dynamics parameterization, based on Bryan [1969]. A more detailed description of the sea ice component can be found in the supporting information.

2.2. Experimental Setup

In order to investigate the impacts of changes to the minimum sea ice albedo (α_{\min}) on simulations of the mid-Pliocene, four simulations with mid-Pliocene boundary conditions were run with α_{\min} values of 0.5 (control), 0.4, 0.3, and 0.2. All used the standard maximum albedo of 0.8. Each simulation was run for 200 years, spun off from an initial 500 year control run, with climatological averages based on the final 30 years. All simulations had achieved equilibrium before 200 years.

In addition to the Pliocene runs, we ran four transient simulations, which started with preindustrial boundary conditions and increased greenhouse gas levels in line with the historic rates up to the present day. Results were compared against historical observations from the Hadley Centre Sea Ice and Sea Surface Temperature (HadISST) data set [Rayner *et al.*, 2003]. The alternative sea ice albedo limits used in the mid-Pliocene simulations were also applied to these runs.

The experimental design uses the template set out in Haywood *et al.* [2011]. All simulations use PRISM3D boundary conditions, at the time of writing the most recent version of the Pliocene Research, Interpretation and Synoptic Mapping (PRISM) paleoenvironmental reconstruction [Dowsett *et al.*, 2010] (see supporting information for more details).

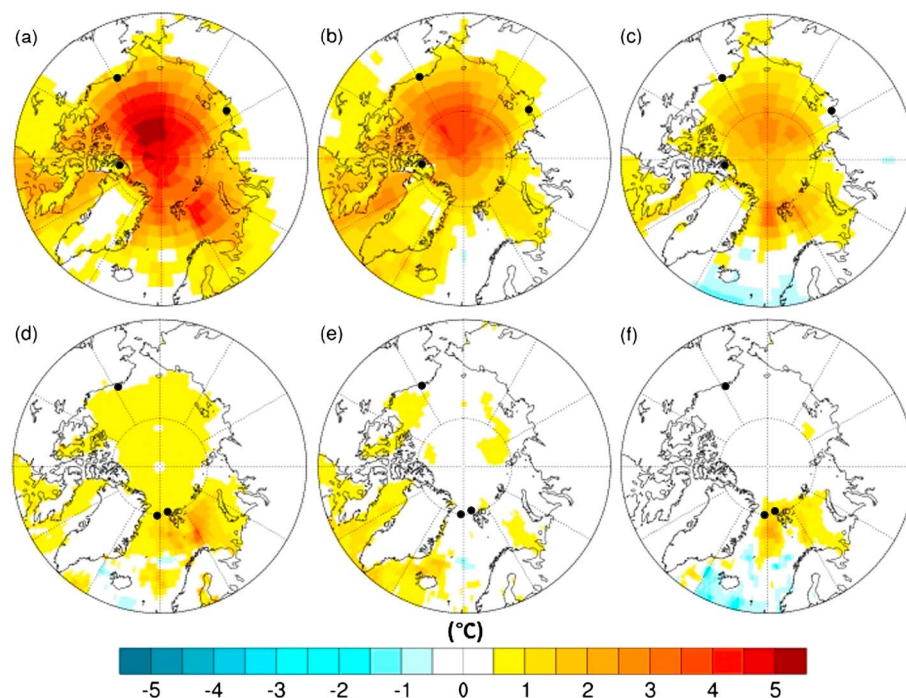


Figure 1. Mean annual temperature ($^{\circ}\text{C}$) anomalies (alternative minus standard) for Pliocene simulations with α_{min} values: (a and d) 0.2, (b and e) 0.3, and (c and f) 0.4. Standard α_{min} is 0.5. Figures 1a–1c show the SAT anomalies, with Figures 1d–1f displaying SST anomalies. Locations of data sites from Tables 1 and 2 are also shown.

2.3. Model-Data Comparisons

To assess the effectiveness of the changes to the sea ice albedo limits on mid-Pliocene model-data mismatches, the model results were compared to mid-Pliocene SAT and SST proxy data temperature estimates. SAT estimates are based on paleobotanical proxy data [Salzmann *et al.*, 2008, 2013], and SST estimates are achieved using multiple proxies, based on Mg/Ca and alkenone paleothermometry and planktonic foraminiferal assemblages [Dowsett *et al.*, 2010, 2013].

We focus on the region north of 60°N . While several SAT and SST data sites outside of this region have large model-data differences, no significant warming is observed in the Northern Hemisphere south of 60°N in our simulations, so these sites display no change in the model-data mismatch. There are nine SAT and five SST data sites north of 60°N [Dowsett *et al.*, 2012; Salzmann *et al.*, 2013]. For each site, we identified the difference between the proxy data estimates and the control simulation temperatures. These are compared with the temperatures produced by the three simulations with reduced minimum albedo. Sites with a model-data mismatch reduction of greater than 0.5°C are presented in the main paper, with the full set published in the supporting information.

3. Results

3.1. Pliocene Albedo Runs

3.1.1. Annual

Figure 1 shows the mean annual SAT and SST anomalies north of 60°N for the simulations with reduced minimum sea ice albedo. Each displays an increase in SAT over the Arctic Ocean, and in most cases this warming spreads across some terrestrial regions. The SAT increase is in excess of 5°C in some areas in the simulation with $\alpha_{\text{min}} = 0.2$.

In comparison with the SAT response, the overall SST response is weaker (Figure 1). A small response is shown for the run with $\alpha_{\text{min}} = 0.2$, with an increase of around 1°C over most of the ocean north of 60°N , with the exception of a region east of Greenland and surrounding Iceland which shows largely no change, as this region was already sea ice free in the standard Pliocene simulation. The simulations with α_{min} reduced to 0.3 and 0.4 show changes of a similar magnitude but cover less area; in the case for $\alpha_{\text{min}} = 0.4$, the change is limited to a small region around the Barents Sea.

Table 1. Pliocene SAT Anomalies (Model-Simulated Temperature Minus Proxy-Reconstructed Temperature) at Three Paleodata Sites^a

Site	Latitude/Longitude	Control Anomaly	$\alpha_{\min} = 0.2$ Anomaly
Beaver Pond	78.40°/−82.00°	−14.51°C	−13.7°C
Ocean Point	70.00°/−153.00°	−8.92°C	−8.2°C
Lena River	72.20°/125.97°	−12.01°C	−11.4°C

^aAnomalies are displayed for the control and $\alpha_{\min} = 0.2$ simulations.

At six of the nine SAT paleodata sites north of 60°N, the temperature change between the control and the $\alpha_{\min} = 0.2$ simulations was less than 0.25°. Table 1 shows the locations of the other three SAT data sites, which all displayed increases of at least 0.5°C in the $\alpha_{\min} = 0.2$ simulation in comparison to the control and the model minus data SAT anomalies for those two simulations at each site. Similarly, two of the five SST data sites north of 60°N displayed temperature differences of less than 0.25°C between the two discussed simulations. Table 2 summarizes the same information for the three remaining SST sites as Table 1 does for the SAT sites. The locations of both the marine and terrestrial sites are displayed in Figures 1 and 2.

3.1.2. Seasonal

Figure 2 shows the four mean seasonal SAT anomalies for the run with $\alpha_{\min} = 0.2$. The largest response is seen in Northern Hemisphere autumn (September–October–November (SON)), where the SAT anomaly is as much as 10°C over some areas of the Arctic. Winter (December–January–February (DJF)) also shows a strong response, with SAT increases over the Arctic Basin of 4–6°C. DJF is the only season where any substantial terrestrial SAT increase is observed. In contrast to SON and DJF, the SAT anomalies in spring (March–April–May (MAM)) and summer (June–July–August (JJA)) are much weaker.

3.2. Transient Runs

Figure 3 shows the Arctic September sea ice extents (area where sea ice concentration is greater than 15%) for the four transient simulations for the historical period, alongside the HadISST sea ice extent observations [Rayner *et al.*, 2003]. Generally, GCMs overestimate the simulation of sea ice extent [Stroeve *et al.*, 2007] in comparison to observations. However, Figure 3 indicates that HadCM3 is an exception and for the majority of the observational period produces a lower September Arctic sea ice extent than observations. The HadCM3 standard simulated sea ice extent does not exceed the observations until into the 21st century, where large declines in September sea ice extent are observed and not reproduced by HadCM3.

All three simulations with reduced minimum albedo produce lower extents than the control and at all points are lower than the observations. Each shows a very rapid initial decline before settling in to a slower downward trend after less than 10 model years. The simulation with $\alpha_{\min} = 0.2$ is intermittently sea ice free from approximately 20 years in to the simulation.

4. Discussion

4.1. Pliocene Albedo Runs

Tables 1 and 2 highlight that although the reduction in the minimum albedo limit has helped produce greater high-latitude warming, it is having a limited effect on reducing the data-model mismatches. Substantial changes are only seen at six data sites, three marine and three terrestrial. Data for these sites are presented in Tables 1 and 2, with the data for all sites north of 60°N presented in Tables S1 and S2 in the supporting information.

The changes are small in comparison to the difference between the model and the data temperatures. For the SATs, the changes represent reductions in the model-data mismatch of just 5 to 8%. All increases are

Table 2. Pliocene SST Anomalies (Model-Simulated Temperature Minus Proxy-Reconstructed Temperature) at Three Paleodata Sites^a

Site	Latitude/Longitude	Control Anomaly	$\alpha_{\min} = 0.2$ Anomaly
Colvillian	70.29°/−150.42°	−2.26°C	−1.61°C
ODP 909	78.58°/−3.07°	−9.82°C	−8.51°C
ODP 911	80.47°/8.23°	−11.14°C	−10.21°C

^aAnomalies are displayed for the control and $\alpha_{\min} = 0.2$ simulations.

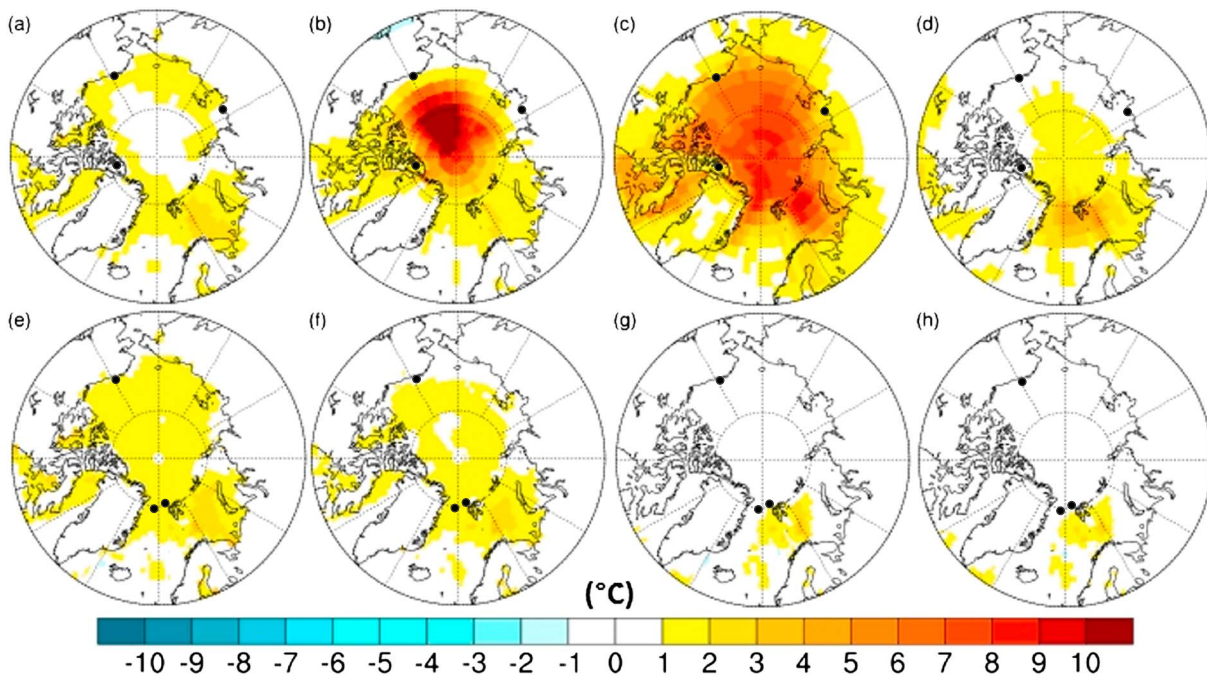


Figure 2. Mean seasonal temperature ($^{\circ}\text{C}$) anomalies (alternative minus standard) for Pliocene simulation with $\alpha_{\min} = 0.2$, showing (a and e) summer (JJA), (b and f) autumn (SON), (c and g) winter (DJF), and (d and h) spring (MAM). Figures 2a–2d show the SAT anomalies, with Figures 2d–2f displaying SST anomalies. Locations of data sites from Tables 1 and 2 are also shown.

within the uncertainty ranges, when provided, for reconstructed SATs [Salzmann *et al.*, 2013]. The largest increases in SAT over the Arctic occurred over the ocean; however, in terrestrial regions, where Pliocene proxy data exist, temperature increases have been much lower.

Lawrence *et al.* [2008] demonstrate, using the Community Climate System Model version 3 (CCSM3), that SAT increases as a result of sea ice loss can penetrate up to 1500 km inland, covering a much larger area than shown in Figures 1 and 2. This suggests that CCSM3 has stronger inland atmospheric heat transport than HadCM3, and therefore, there is an element of model dependency on the extent to which the SAT anomalies are reduced. A similar set of simulations performed with a model such as CCSM3 with stronger inland heat

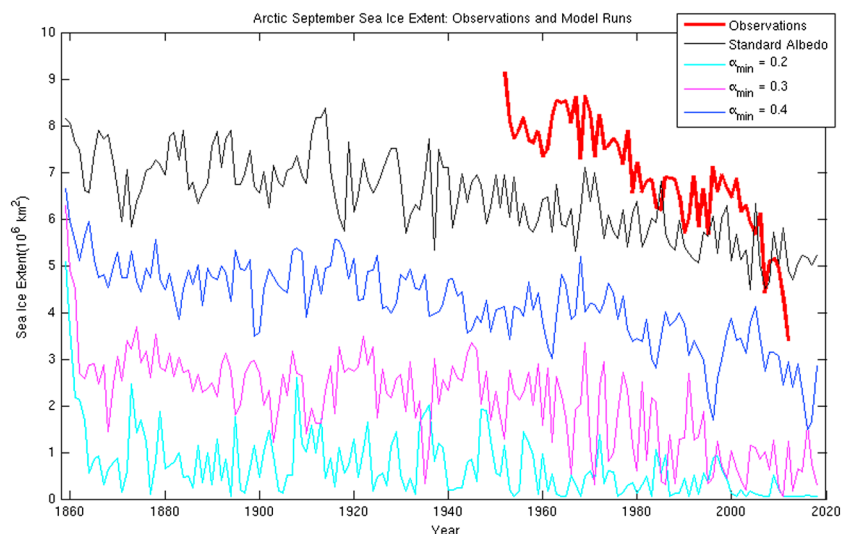


Figure 3. Arctic September sea ice extent (10^6 km^2) from observations (thick red line) and 4 HadCM3 transient simulations with varying minimum sea ice albedos.

penetration may prove more effective at reducing the data-model discrepancies than HadCM3 has shown in this study.

The PRISM time slab covers a period of up to 300,000 years, during which the orbital configurations varied substantially. It is not clear whether the proxy data are representative of the orbital configuration used in the experiment (identical to modern) or whether they may be indicating temperatures from times with the warmest orbital configurations of the time slab.

Salzmann et al. [2013] ran a simulation under Pliocene Model Intercomparison Project boundary conditions with orbital configurations adjusted to ensure maximum Pliocene top of the atmosphere incoming insolation 65°N in July, based on the astronomical solution of *Laskar et al.* [2004]. Figure S7 shows the SAT differences between this simulation (Pliocene Northern Hemisphere Maximum (NH Max)) and the simulation with $\alpha_{\text{min}} = 0.2$. The Pliocene NH Max simulation unsurprisingly produces higher SATs at mid-latitudes in spring and summer, as the orbit was picked to produce the maximum summer insolation at 65°N , and there is little warming produced at these latitudes by reducing α_{min} . However, the simulation with $\alpha_{\text{min}} = 0.2$ produces much higher SAT increases in autumn and winter over the region north of 60°N .

Figure S8 demonstrates that with the exception of part of the Bering Sea in winter and spring, the Pliocene NH Max simulation does not melt more sea ice than the $\alpha_{\text{min}} = 0.2$ simulation. The difference is particularly striking in the autumn months, where the Pliocene NH Max simulation does not produce the large sea ice reduction seen in the $\alpha_{\text{min}} = 0.2$ simulation. The effects of the combination of these two factors will be tested in a future study.

While the overall SST response was weaker than the SAT response, the changes highlighted in Tables 1 and 2 show a slightly greater increase on average for the SST data sites. These changes resulted in reductions in the model-data mismatch of 8 to 29%, much higher than for the SATs, although this is partly due to the initial SAT differences being much larger. Similar to the SATs, all SST changes are less than the errors associated to the techniques used to reconstruct the Pliocene temperatures [*Dowsett et al.*, 2009].

The counterintuitive seasonal SAT warming pattern, seen in Figure 2, has been previously observed in modeling and observational studies [*Kumar et al.*, 2010; *Screen and Simmonds*, 2010a, 2010b], which look at the effects of declining Arctic sea ice cover. It is suggested that the pattern is caused when the increased heat absorbed by the ocean in summer due to sea ice loss is released over the autumn and winter as the sea ice recovers. The simulation with $\alpha_{\text{min}} = 0.2$ sees a 55% decrease in sea ice fraction in JJA, and an 89% decrease in SON, suggesting that the seasonal warming pattern of this simulation is also due to a large decrease in sea ice cover. Further discussion of this pattern is found in the supporting information.

4.2. Transient Runs

While all simulations underestimated late twentieth century sea ice extent, results for the 21st century show the observations declining faster than the HadCM3 standard simulation (Figure 3). The HadCM3 sea ice extent continues the same downward trend in the 21st century that it displays for the twentieth, in comparison to the accelerated decline seen in the observations, implying that the two will continue to diverge. As the September sea ice extent declines further, an increasing proportion of the sea ice cover will be first-year ice, which has a lower albedo than multiyear ice [*Perovich and Polashenski*, 2012; *Polashenski et al.*, 2012]. This may imply that a different sea ice albedo setup (with a lower minimum value) would be more appropriate for future simulations than one better suited to a climate with a greater proportion of multiyear ice.

Figure 3 demonstrates that there are problems using any fixed minimum sea ice albedo. While the standard HadCM3 setup appears unsuitable for simulating 21st century sea ice, the simulations with reduced albedo produce sea ice extents substantially below observations. A more sophisticated parameterization, allowing the minimum sea ice albedo to vary depending on the age of the ice, could enable the model to match the observations more closely. However, this would require the inclusion of a tracer for sea ice age into the model [e.g., *Hunke and Bitz*, 2009], a level of sophistication beyond the capabilities of HadCM3. More modern models, such as CCSM4, implement shortwave radiation parameterizations to simulate the surface albedo, rather than basing it on bulk sea ice properties such as surface temperatures [*Holland et al.*, 2012]. The greater capabilities of these models highlights a disadvantage to using an older model such as HadCM3, although as *Koenigk et al.* [2013] demonstrates, CCSM4 still does not achieve the low albedos observed in *Perovich and Polashenski* [2012].

The divergence of the control HadCM3-simulated September sea ice extent and the observations in the 21st century shown in Figure 3 are a clear indication that the standard sea ice albedo settings are not suitable for simulating warmer climates with a higher proportion of first-year ice. As proxy data indicate that high-latitude mid-Pliocene SSTs were warmer than those at the present day [Dowsett *et al.*, 2010], then it is not unreasonable to infer that mid-Pliocene Arctic sea ice cover would have been diminished, with less sea ice surviving the summer. The sea ice would therefore have been dominated by first-year ice, and consequently a different albedo parameterization, enabling a lower minimum, would be more suitable for mid-Pliocene simulations.

5. Conclusions

This paper has demonstrated the capabilities and limitations of the influence of the sea ice albedo feedback. The use of a lower sea ice albedo limit, one more suitable for a warmer than present-day climate with almost certainly less multiyear ice, has led to mean annual SAT increases of up to 6°C over the Arctic Ocean. However, the effect on mid-Pliocene model-data mismatches is much smaller. Any changes in these mismatches are small in comparison to the overall model-data temperature differences and are within the uncertainty ranges of the temperature reconstruction for each site, when provided [Salzmann *et al.*, 2013]. The maximum changes seen in data-model mismatches for SSTs are slightly higher than for SATs, despite the overall response being much weaker; however, these changes are also less than the uncertainty ranges for the reconstructed temperatures [Dowsett *et al.*, 2009].

These results suggest that temperature increases large enough to eliminate the model-data mismatch, particularly for SATs, are unlikely to be solely driven by ocean-based changes to the model, except in extreme scenarios such as the complete removal of Pliocene Arctic sea ice [e.g., Ballantyne *et al.*, 2013]. The changes made to the minimum sea ice albedo can be considered a useful tool in helping to close this gap, but they can only be part of a larger effort.

The transient simulations highlight an area in which the albedo changes have had a particularly dramatic effect. There is a large sea ice reduction in autumn in the Pliocene simulations, and this is replicated in the transient runs, resulting in a large difference in the September sea ice extent minimum in comparison to the control. The failure of the HadCM3 standard parameterization to reproduce the recent sea ice decline suggests that it is not suited to simulating climates with higher proportions of first-year sea ice. Currently, there are insufficient data to say with any certainty whether the alternative sea ice albedo minima will simulate 21st century Arctic sea ice better. However, these alternative albedo limits would appear to have a greater chance at replicating the rapid downward trend seen in the observations than the standard settings.

Acknowledgments

F.W.H. and J.O.P. acknowledge NERC for the provision of doctoral training grants. A.M.H., A.M.D., and S.J.P. acknowledge that funding for this research was partly provided by a European Research Council starting grant under agreement 278636. D.J.H. is funded by a Leverhulme Early Career Fellowship (ECF-2011-205) and financially supported by the British Geological Survey and National Centre for Atmospheric Science. H.J.D. acknowledges the continued support of the U.S. Geological Survey Climate and Land Use Change Research and Development Program. U.S. acknowledges financial support from the Natural Environment Research Council (NE/I016287/1). This research used samples and/or data provided by the Integrated Ocean Drilling Program. We thank the reviewers for their comments, which helped to improve the manuscript.

The Editor thanks two anonymous reviewers for their assistance in evaluating this paper.

References

- Ballantyne, A. P., Y. Axford, G. H. Miller, B. L. Otto-Bliesner, N. Rosenbloom, and J. W. C. White (2013), The amplification of Arctic terrestrial surface temperatures by reduced sea-ice extent during the Pliocene, *Palaeogeogr. Palaeoclimatol. Palaeoecol.*, *386*, 59–67, doi:10.1016/j.palaeo.2013.05.002.
- Bryan, K. (1969), Climate and the ocean circulation III: The ocean model, *Mon. Weather Rev.*, *97*(11), 806–827.
- Cattle, H., and J. Crossley (1995), Modelling Arctic climate change, *Philos. Trans. R. Soc. London, Ser. A*, *352*(1699), 201–213, doi:10.1098/rsta.1995.0064.
- Comiso, J. C., C. L. Parkinson, R. Gersten, and L. Stock (2008), Accelerated decline in the Arctic sea ice cover, *Geophys. Res. Lett.*, *35*, L01703, doi:10.1029/2007GL031972.
- Cronin, T. M., R. Whatley, A. Wood, A. Tsukagoshi, N. Ikeya, E. M. Brouwers, and W. M. Briggs Jr. (1993), Microfaunal evidence for elevated Pliocene temperatures in the Arctic Ocean, *Paleoceanography*, *8*(2), 161–173, doi:10.1029/93PA00060.
- Curry, J. A., J. L. Schramm, and E. E. Ebert (1995), Sea ice-albedo climate feedback mechanism, *J. Clim.*, *8*(2), 240–247, doi:10.1175/1520-0442(1995)008<0240:SIACFM>2.0.CO;2.
- Dowsett, H. J., M. A. Chandler, and M. M. Robinson (2009), Surface temperatures of the mid-Pliocene North Atlantic Ocean: Implications for future climate, *Philos. Trans. R. Soc. London, Ser. A*, *367*(1886), 69–84, doi:10.1098/rsta.2008.0213.
- Dowsett, H., M. Robinson, A. Haywood, U. Salzmann, D. Hill, L. Sohl, M. Chandler, M. Williams, K. Foley, and D. Stoll (2010), The PRISM3D paleoenvironmental reconstruction, *Stratigraphy*, *7*(2-3), 123–139.
- Dowsett, H. J., A. M. Haywood, P. J. Valdes, M. M. Robinson, D. J. Lunt, D. Hill, D. K. Stoll, and K. M. Foley (2011), Sea surface temperatures of the mid-Piacenzian Warm Period: A comparison of PRISM3 and HadCM3, *Palaeogeogr. Palaeoclimatol. Palaeoecol.*, *309*(1-2), 83–91, doi:10.1016/j.palaeo.2011.03.016.
- Dowsett, H. J., et al. (2012), Assessing confidence in Pliocene sea surface temperatures to evaluate predictive models, *Nat. Clim. Change*, *2*(5), 365–371, doi:10.1038/nclimate1455.
- Dowsett, H. J., et al. (2013), Sea surface temperature of the mid-Piacenzian Ocean: A data-model comparison, *Sci. Rep.*, *3*, doi:10.1038/srep02013.
- Eisenman, I., N. Untersteiner, and J. S. Wettlaufer (2008), Reply to comment by E. T. DeWeaver et al. on "On the reliability of simulated Arctic sea ice in global climate models", *Geophys. Res. Lett.*, *35*, L04502, doi:10.1029/2007GL032173.

- Gordon, C., C. Cooper, C. A. Senior, H. Banks, J. M. Gregory, T. C. Johns, J. F. B. Mitchell, and R. A. Wood (2000), The simulation of SST, sea ice extents and ocean heat transports in a version of the Hadley Centre coupled model without flux adjustments, *Clim. Dyn.*, *16*(2-3), 147–168, doi:10.1007/s003820050010.
- Haywood, A. M., and P. J. Valdes (2004), Modelling Pliocene warmth: Contribution of atmosphere, oceans and cryosphere, *Earth Planet. Sci. Lett.*, *218*(3-4), 363–377, doi:10.1016/S0012-821X(03)00685-X.
- Haywood, A. M., H. J. Dowsett, M. M. Robinson, D. K. Stoll, A. M. Dolan, D. J. Lunt, B. L. Otto-Bliesner, and M. A. Chandler (2011), Pliocene Model Intercomparison Project (PlioMIP): Experimental design and boundary conditions (experiment 2), *Geosci. Model Dev.*, *4*, 571–577, doi:10.5194/gmd-4-571-2011.
- Haywood, A. M., et al. (2013), Large-scale features of Pliocene climate: Results from the Pliocene Model Intercomparison Project, *Clim. Past*, *9*(1), 191–209, doi:10.5194/cp-9-191-2013.
- Hibler, W. D. (1979), A dynamic-thermodynamic sea ice model, *J. Phys. Oceanogr.*, *9*, 815–846.
- Holland, M. M., D. A. Bailey, B. P. Briegleb, B. Light, and E. Hunke (2012), Improved sea ice shortwave radiation physics in CCSM4: The impact of melt ponds and aerosols on Arctic sea ice, *J. Clim.*, *25*(5), 1413–1430, doi:10.1175/JCLI-D-11-00078.1.
- Hunke, E. C., and C. M. Bitz (2009), Age characteristics in a multidecadal Arctic sea ice simulation, *J. Geophys. Res.*, *114*, C08013, doi:10.1029/2008JC005186.
- Hunke, E. C. (2010), Thickness sensitivities in the CICE sea ice model, *Ocean Modell.*, *34*(3-4), 137–149, doi:10.1016/j.ocemod.2010.05.004.
- Intergovernmental Panel on Climate Change (IPCC) (2007), *Climate Change 2007: The Physical Science Basis. Contribution of Working Group I to the Fourth Assessment Report of The Intergovernmental Panel on Climate Change*, edited by S. Solomon et al., 906 pp., Cambridge Univ. Press, Cambridge, U. K., and New York.
- Kellogg, W. W. (1975), Climatic feedback mechanisms involving the polar regions, in *Climate of the Arctic*, edited by G. Weller and S. A. Bowling, pp. 111–116, Geophysical Institute, Fairbanks, Alaska.
- Koenig, T., A. Devasthale, and K. G. Karlsson (2013), Summer sea ice albedo in the Arctic in CMIP5 models, *Atmos. Chem. Phys. Discuss.*, *13*(9), 25219–25251, doi:10.5194/acpd-13-25219-2013.
- Kumar, U., J. Perlwitz, J. Eischeid, X. W. Quan, T. Y. Xu, T. Zhang, M. Hoerling, B. Jha, and W. Q. Wang (2010), Contribution of sea ice loss to Arctic amplification, *Geophys. Res. Lett.*, *37*, L21701, doi:10.1029/2010GL045022.
- Laskar, J., P. Robutel, F. Joutel, M. Gastineau, A. C. M. Correia, and B. Levrard (2004), A long-term numerical solution for the insolation quantities of the Earth, *Astron. Astrophys.*, *428*(1), 261–285, doi:10.1051/0004-6361:20041335.
- Lawrence, D. M., A. G. Slater, R. A. Tomas, M. M. Holland, and C. Deser (2008), Accelerated Arctic land warming and permafrost degradation during rapid sea ice loss, *Geophys. Res. Lett.*, *35*, L11506, doi:10.1029/2008GL033985.
- Maykut, G. A. (1978), Energy exchange over young sea ice in the central Arctic, *J. Geophys. Res.*, *83*(C7), 3646–3658, doi:10.1029/JC083iC07p03646.
- Moran, K., et al. (2006), The Cenozoic palaeoenvironment of the Arctic Ocean, *Nature*, *441*(7093), 601–605, doi:10.1038/nature04800.
- Pagani, M., Z. Liu, J. LaRiviere, and A. C. Ravelo (2010), High Earth-system climate sensitivity determined from Pliocene carbon dioxide concentrations, *Nat. Geosci.*, *3*(1), 27–30, doi:10.1038/ngeo724.
- Perovich, D. K., S. V. Nghiem, T. Markus, and A. Schweiger (2007), Seasonal evolution and interannual variability of the local solar energy absorbed by the Arctic sea ice-ocean system, *J. Geophys. Res.*, *112*, C03005, doi:10.1029/2006JC003558.
- Perovich, D. K., and C. Polashenski (2012), Albedo evolution of seasonal Arctic sea ice, *Geophys. Res. Lett.*, *39*, L08501, doi:10.1029/2012GL051432.
- Polashenski, C., D. Perovich, and Z. Courville (2012), The mechanisms of sea ice melt pond formation and evolution, *J. Geophys. Res.*, *117*, C01001, doi:10.1029/2011JC007231.
- Polyak, L., et al. (2010), History of sea ice in the Arctic, *Quat. Sci. Rev.*, *29*(15-16), 1757–1778, doi:10.1016/j.quascirev.2010.02.010.
- Rayner, N. A., D. E. Parker, E. B. Horton, C. K. Folland, L. V. Alexander, D. P. Rowell, E. C. Kent, and A. Kaplan (2003), Global analyses of sea surface temperature, sea ice, and night marine air temperature since the late nineteenth century, *J. Geophys. Res.*, *108*(D14), 4407, doi:10.1029/2002JD002670.
- Salzmann, U., A. M. Haywood, D. J. Lunt, P. J. Valdes, and D. J. Hill (2008), A new global biome reconstruction and data-model comparison for the Middle Pliocene, *Global Ecol. Biogeogr.*, *17*(3), 432–447, doi:10.1111/j.1466-8238.2008.00381.x.
- Salzmann, U., et al. (2013), Challenges in quantifying Pliocene terrestrial warming revealed by data-model discord, *Nat. Clim. Change*, *3*, 969–974, doi:10.1038/nclimate2008.
- Screen, J. A., and I. Simmonds (2010a), The central role of diminishing sea ice in recent Arctic temperature amplification, *Nature*, *464*(7293), 1334–1337, doi:10.1038/nature09051.
- Screen, J. A., and I. Simmonds (2010b), Increasing fall-winter energy loss from the Arctic Ocean and its role in Arctic temperature amplification, *Geophys. Res. Lett.*, *37*, L16707, doi:10.1029/2010GL044136.
- Seki, O., G. L. Foster, D. N. Schmidt, A. Mackensen, K. Kawamura, and R. D. Pancost (2010), Alkenone and boron-based Pliocene pCO₂ records, *Earth Planet. Sci. Lett.*, *292*(1-2), 201–211, doi:10.1016/j.epsl.2010.01.037.
- Semtner, A. J. (1976), A model for the thermodynamic growth of sea ice in numerical investigations of climate, *J. Phys. Oceanogr.*, *6*, 379–389.
- Stroeve, J., M. M. Holland, W. Meier, T. Scambos, and M. Serreze (2007), Arctic sea ice decline: Faster than forecast, *Geophys. Res. Lett.*, *34*, L09501, doi:10.1029/2007GL029703.
- Stroeve, J. C., V. Kattsov, A. Barrett, M. Serreze, T. Pavlova, M. Holland, and W. N. Meier (2012), Trends in Arctic sea ice extent from CMIP5, CMIP3 and observations, *Geophys. Res. Lett.*, *39*, L16502, doi:10.1029/2012GL052676.